Quantitative susceptibility imaging of the rat brain using a dedicated setup allowing different orientations along B0

L. de Rochefort[1], T. Liu[2], M. Guillemiller[1], D. Houitte[1], Y. Wang[2], P. Hantraye[1], and V. Lebon[1]

[1]MIRCen, CEA-CNRS, Fontenay-aux-roses, France, [2]Radiology, Weill Medical College of Cornell University, New York, NY, United States

INTRODUCTION

MR imaging of tissue susceptibility is a promising approach for exploring various pathological conditions such as neurodegenerative processes associated with iron deposition, aggregate or contrast agent accumulation (1). Quantitative mapping of susceptibility uses the magnetic field induced by susceptibility to quantify the magnetic sources. This challenging ill-posed inversion problem (2) requires both dedicated acquisition protocols and regularization procedures (2-7). The inversion can be stabilized by including data from many object orientations with respect to B_0. In this study we developed a dedicated setup allowing MR acquisition of the rat brain along 2 different orientations along B_0. Field map and susceptibility maps were derived from MR phase images, demonstrating the ability to quantify magnetic susceptibility in the rat brain.

MATERIAL AND METHODS

MR system Experiments were performed on a horizontal 7T/40cm system (Varian, Palo Alto, CA) equipped with a 30cm ID gradient coil (80 mT/m). A dedicated rat holder was designed to allow precise rotation of the rat along the vertical axis Y of the magnet by 45° (pivot axis on Fig.1). RF transmission at 299.43MHz was performed using a 10cm diameter Helmholtz coil (main axis along Y). A 2-channel surface coil was placed on the rat head for reception. Note that transmitted and detected B1 were along Y, making both transmit power and detection insensitive to the rat rotation along Y. Both RF coils were actively decoupled.

Animal handling A 300g male Sprague Dawley rat was anesthetized by i.p. injection of Ketamine Domitor. The rat was immobilized in a prone position using ear rods and tooth bar. After shimming and scout imaging, 32 2D slices were acquired with a spoiled gradient echo sequence for 6 different echo times. Parameters were: 125µmx125µm in plane resolution (24x32mm FOV, 192x256MTX), 500µm slice thickness, 50 kHz SW, TR/TEs=1s/4.9, 5.9, 7.9, 11.9, 19.9, 25.9ms. A first dataset was acquired with the rat aligned along B_0 (0° image). Then the setup was rotated by 45° along Y and a second dataset was acquired (45° image).

Image processing Field maps were reconstructed by fitting the phase evolution with TE. A high-pass filter was then applied similar to susceptibility weighted imaging by removing the phase of a low pass filtered image (Gaussian filter in image space). The 45° image was rotated and registered to the 0° image. A mask was applied to separate the brain region. Filtered field maps were then processed on a limited region of the brain for a susceptibility reconstruction χ. The least-square minimization problem was written as follows: $\min_{\chi,\varepsilon} \|W\,(C\chi - B/B_0)\|_2^2 + \|W\,(C_{45}\chi - B_{45}/B_0)\|_2^2 + \alpha\,\|M\chi\|_2^2 + \beta\,\|G\chi\|_2^2$

The two first terms are squared distances between the measured fields along 0 and 45°, B/B_0 and B_{45}/B_0, and the fitted ones $C\chi$ and $C_{45}\chi$ for each orientation. The third and forth terms are regularization terms on the susceptibility and its gradient, respectively. M is a mask defining a region at the domain boundaries to force a reference region. G is the gradient operator which is used to impose smoothness of the solution. A conjugate gradient algorithm was used to perform the regularized inversion.

RESULTS

Increasing T2* effects were observed with increasing TE as expected (Fig. 2). The field showed strong dependence on orientation (Fig.3) with drastically changing patterns between 0 and 45°. Patterns tend to follow large vessels. The phase tends to vanish when vessels are aligned along B_0 and to increase when perpendicular (Fig. 3a). For vessels perpendicular to B_0 and to the imaging slice (Fig. 3b), the orientation of dipolar patterns along B_0 was preserved after 45° brain rotation, i.e. dipolar pattern rotated in the rat brain. Corresponding susceptibility maps indicate paramagnetic regions (Fig.4).

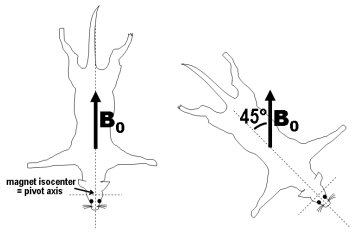

Fig. 1: Experimental setup. The rat orientation with respect to the magnetic field was varied centered on brain.

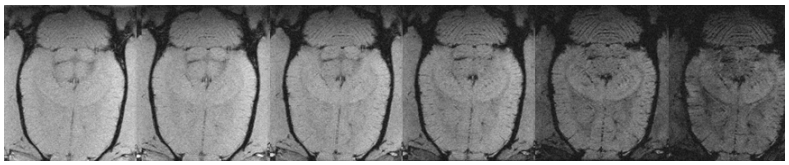

Fig. 2: Six echoes obtained for one slice displays increasing T2* effects.

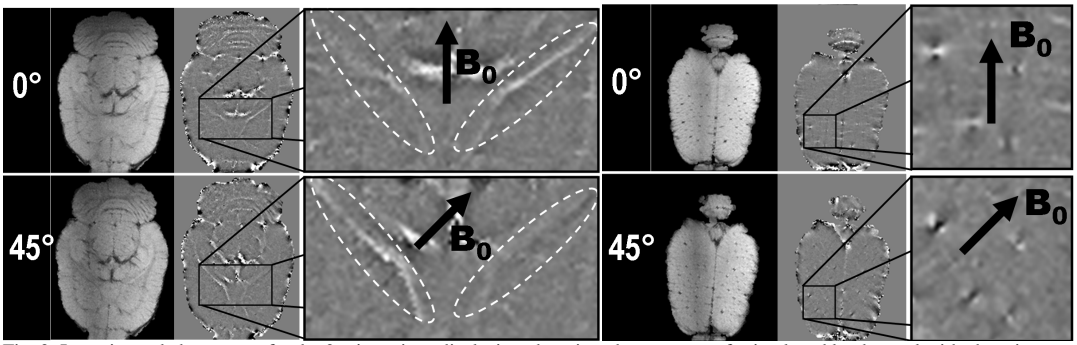

Fig. 3: Intensity and phase maps for the 2 orientations displaying changing phase patterns for in plane blood vessel with changing orientation along B_0 (left). Dipolar field patterns for through plane blood vessels (right). Note the changing orientation of the dipole fields.

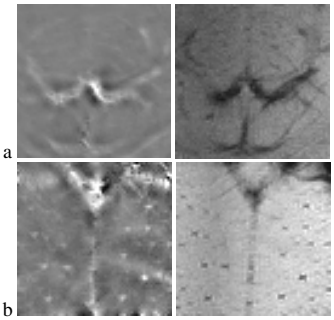

Fig. 4: Susceptibility maps obtained with α=1000 and β=250 for a central slice (a, same as Fig.3left) and a higher slice (b, Fig.3 right), as well as corresponding intensity map (right)

DICUSSION AND CONCLUSION

Field maps showing dipolar effects induced by susceptibility were obtained in vivo at 7T, using a dedicated setup allowing acquisition of multiple orientations along B_0. Field maps exhibited high contrast around blood vessels with a strong dependence on B_0 direction. Susceptibility maps were reconstructed from these data. The presented protocol opens a way for quantitative susceptibility mapping using multiple orientation sampling (4). Our preliminary results illustrate the possibility of mapping paramagnetic vessels in vivo in the rat brain. Improvements are needed to optimally reconstruct susceptibility maps such as increasing phase SNR, registering data from the multiple orientations and assessing the effects of filtering used to remove long range susceptibility effects. This approach could be used to quantify iron deposition in the brain or iron-oxides particle distribution used for cellular/molecular MRI.

REFERENCES 1. Haacke et al., MRI 23p1**, 2.** de Rochefort et al., MRM 60p1003 **3.** Kressler et al. ISMRM 2008 p 1514 **4.** Liu et al., ISMRM 2008 p 643 **5.** Hammond et al., ISMRM 2008 p 1512 **6.** Shmueli et al., ISMRM 2008 p642 **7.** Schafer et al., ISMRM 2008 p641